

# RSC Advances



This is an *Accepted Manuscript*, which has been through the Royal Society of Chemistry peer review process and has been accepted for publication.

*Accepted Manuscripts* are published online shortly after acceptance, before technical editing, formatting and proof reading. Using this free service, authors can make their results available to the community, in citable form, before we publish the edited article. This *Accepted Manuscript* will be replaced by the edited, formatted and paginated article as soon as this is available.

You can find more information about *Accepted Manuscripts* in the [Information for Authors](#).

Please note that technical editing may introduce minor changes to the text and/or graphics, which may alter content. The journal's standard [Terms & Conditions](#) and the [Ethical guidelines](#) still apply. In no event shall the Royal Society of Chemistry be held responsible for any errors or omissions in this *Accepted Manuscript* or any consequences arising from the use of any information it contains.

## Ohmic Contacts of ZnO/SnO<sub>2</sub> Equal-cosubstituted In<sub>2</sub>O<sub>3</sub> Films to n-InP and p-GaAs

Xiufeng Tang<sup>a,b,\*</sup>, Chunhan Hseih<sup>a</sup>, Fang Ou<sup>a</sup> and Seng-Tiong Ho<sup>a</sup>

<sup>a</sup> *Department of Electrical Engineering and Computer Science, Northwestern University, Evanston, Illinois 60208, United States*

<sup>b</sup> *State Key Laboratory of Solidification Processing, School of Materials Science and Engineering, Northwestern Polytechnical University, Xi'an 710072, China;*

\* Corresponding author. Tel.: (+86) 029-88494574;

E-mail address:

Xiufeng Tang: [tbrenda@sina.com](mailto:tbrenda@sina.com)

Chunhan Hseih: [chunhanhseih2013@u.northwestern.edu](mailto:chunhanhseih2013@u.northwestern.edu)

Seng-Tiong Ho: [sth@northwestern.edu](mailto:sth@northwestern.edu)

## Abstract

ZnO/SnO<sub>2</sub> equal-cosubstituted In<sub>2</sub>O<sub>3</sub> (ZITO) films were deposited by ion beam assisted deposition onto n-InP and p-GaAs substrates. Rapid contact annealing processes (RCP) at different temperatures were done to study the thermal stability of their interfacial contact properties between ZITO films and the semiconductor substrates. Oxygen flow rate during deposition is the main tuning parameter for ZITO films growth. Highest conductivity for ZITO film deposited at the oxygen flow rate of 0 sccm (ZITO-0) was got at 525.2 S/cm; lowest optical loss at wavelength of 1550 nm for ZITO film prepared at the oxygen flow rate of 7 sccm (ZITO-7) was obtained at 592.7 cm<sup>-1</sup>. Ohmic contacts have been achieved between ZITO films and n-InP pretreated both by hydrogen plasma and by oxygen plasma (H<sub>2</sub>-cleaned n-InP and O<sub>2</sub>-cleaned n-InP). The contact between ZITO-0 film and H<sub>2</sub>-cleaned n-InP substrate shows good thermal stability in RCP, the specific contact resistivity of 1.84×10<sup>-4</sup> Ω.cm<sup>2</sup> for as-deposited ZITO-0 film contact to H<sub>2</sub>-cleaned n-InP and 1.24×10<sup>-4</sup> Ω.cm<sup>2</sup> for the one annealed at 450 °C. While, RCP at proper temperature (360 °C and 400 °C) is the key to achieve Ohmic contact between ZITO-0 film to H<sub>2</sub>-cleaned p-GaAs substrate.

**Keywords:** Ohmic contact, ZITO film, substrate surface pretreatment, rapid contact annealing process

## 1. Introduction

Transparent conducting oxides (TCOs) have attracted much attention for decades due to the increasing needs for their concurrent properties of electrical conductivity and optical transparency [1-4]. One of the important characteristics in  $\text{In}_2\text{O}_3$  cosubstituted with  $\text{ZnO}$  and  $\text{SnO}_2$  in equal molar amounts is that their respective solubility can be greatly increased to about 20% for each [5, 6], while the solubility for individual doping is less than 1% and about 6% respectively [7, 8]. The cosubstitution of  $\text{ZnO}$  and  $\text{SnO}_2$  creates a net-isovalent substitution pair of  $2\text{In}_2\text{O}_3$  and has used to create new TCO materials,  $\text{In}_{2-2x}\text{Zn}_x\text{Sn}_x\text{O}_3$  [5, 6, 9, 10]. When cosubstituted in equal molar amounts throughout the solubility range, the cubic bixbyite structure of crystal  $\text{In}_2\text{O}_3$  is retained as the lattice parameter contracts from  $10.120 \text{ \AA}$  to  $9.994 \text{ \AA}$ , which is consistent with ionic radii of the cosubstituted species [5, 11]. Both  $\text{Zn}^{2+}$  ( $0.740 \text{ \AA}$ ) and  $\text{Sn}^{4+}$  ( $0.690 \text{ \AA}$ ) have smaller 6-coordinate ionic radii than  $\text{In}^{3+}$  ( $0.800 \text{ \AA}$ ) [5].

There is much study on equal-cosubstituted ZITO reported. G. B. Palmer [5] reported a conductivity of over 500 S/cm to 2575 S/cm for reduced bulk  $\text{In}_{2-2x}\text{Zn}_x\text{Sn}_x\text{O}_3$  with  $x=0\sim 0.4$  and the conductivity generally decreased with the increasing cosubstitution concentration. A. Ambrosini [6] showed that carrier concentrations and mobilities for the unreduced cosubstituted bulk  $\text{In}_{2-2x}\text{Zn}_x\text{Sn}_x\text{O}_3$  are  $1.7\sim 3.0 \times 10^{20} \text{ cm}^{-3}$  and  $18\sim 31 \text{ cm}^2/\text{V.s}$  respectively and for reduced samples are  $3.2\sim 7.0 \times 10^{20} \text{ cm}^{-3}$  and  $13\sim 14 \text{ cm}^2/\text{V.s}$ . As to equal-cosubstituted ZITO films, M. Zhang [9] prepared crystalline  $\text{Zn}_{0.3}\text{In}_{1.4}\text{Sn}_{0.3}\text{O}_{3-\delta}$  films ( $x=0.3$ ) by pulsed laser deposition (PLD) on (0001)  $\text{Al}_2\text{O}_3$  substrates and the as-deposited ZITO film showed a conductivity of 2516 S/cm, a carrier concentration of

$3.9 \times 10^{20} \text{ cm}^{-3}$  with n-type transport, and a mobility of  $39.7 \text{ cm}^2/\text{V.s}$ . Besides, also by PLD, D. Bruce Buchholz [10] prepared amorphous ZITO films from a target with the composition of  $\text{In}_{1.40}\text{Zn}_{0.33}\text{Sn}_{0.27}\text{O}_3$  and reported a conductivity of  $1700 \text{ S/cm}$ , a carrier concentration of  $3 \times 10^{20} \text{ cm}^{-3}$  and a mobility of  $36 \text{ cm}^2/\text{V.s}$ . Especially, low refractive index  $n=1.85 \pm 0.1$  and lower optical loss coefficient than ITO in the near infra-red region were reported by Julia M. Phillips [12]. ZITO is therefore a promising material for application in III-V semiconductor optoelectronics and photonic devices working in near infrared wavelength that require transparent electrodes. Good electrical and optical properties and low refractive index relative to InP ( $n \approx 3.2$ ) and GaAs ( $n \approx 3.4$ ) gift ZITO films good possibility that they could be used as a conducting waveguide cladding material for current injection into high refractive index contrast nanophotonic devices [13,14]. However, there isn't much reported regarding the electrical contact properties of ZITO with III-V semiconductors such as InP and GaAs that are often used in such devices. Critical concerns for these applications are the optimization between the electrical conductivity and the optical loss of bulk ZITO films, and the interfacial electrical contact property and its thermal stability of ZITO films and semiconductor substrates in the post-deposition contact annealing process. Good Ohmic contact with minimized contact resistance and its good thermal stability in post-deposition annealing process are critically necessary.

Previously, CdO films and  $\text{In}_2\text{O}_3$  films were ever studied as transparent electrodes and Ohmic contacts with low contact resistance to n-InP substrates were obtained [15, 16]. However, CdO is toxic and the electrical conductivity of  $\text{In}_2\text{O}_3$  is relatively poor. Equal-cosubstituted ZITO based on the literature research could possess superior

properties to CdO or In<sub>2</sub>O<sub>3</sub>.

In this study, zinc-indium-tin oxide (ZITO) films were prepared by ion beam assisted deposition (IAD), in which about 40% of the indium in the In<sub>2</sub>O<sub>3</sub> structure is replaced by substitution with zinc and tin in equal molar proportions: In<sub>2-2x</sub>Zn<sub>x</sub>Sn<sub>x</sub>O<sub>3-δ</sub>, where x=0.4. The oxygen flow rate during deposition is the main tuning parameter for films growth and its effects on optical and electrical properties of ZITO films were discussed. The electrical contact properties across the interface between the contact material, ZITO, and the semiconductor, n-InP and p-GaAs were investigated. Prior to film deposition, hydrogen or oxygen plasma pretreatments were done on n-InP and p-GaAs substrates to remove C, N contaminants, which were also expected to change the effective surface state of semiconductor substrates [17], with the passivation effect of atomic hydrogen by terminating the surface dangling bond [18,19] and the activation effect of O-plasma treatment by improvement of the surface work function resulting from the increase of oxygen concentration on the surface [20,21]. In addition, rapid contact annealing processes (RCP) around 360 °C to 450 °C were carried out and thermal stability of the interfacial contacts was discussed.

## 2. Experimental

### 2.1 Film preparation

ZITO films were prepared at room temperature using Ion-Assisted Deposition (IAD, ION TECH, INC, USA) with SnO<sub>2</sub> 17.5 at.% - In<sub>2</sub>O<sub>3</sub> 28.75 at.% - ZnO 25 at.% target (99.99 % pure, Kurt J. Lesker company). Prior to deposition, all substrates were first solvent cleaned in 3 minutes of ultrasonic bath sequentially in acetone, IPA (Isopropyl Alcohol), and then deionized water; substrates cleaned by this method are referred to as

solvent-cleaned samples. Some substrates were further cleaned by reactive ion etching (RIE) in Oxygen and others in Hydrogen ( $O_2$  or  $H_2$ , 50 mtorr, 100 W, 1 min). Samples received surface treatments of RIE plasma cleaning are referred to as  $O_2$ -cleaned or  $H_2$ -cleaned. All samples were directly put into IAD apparatus right after ex-situ pretreatments and the elapse was shortened to be less than 10 min to avoid contamination again.

During deposition, local temperature of the sample was stabilized by cooling water to be less than  $50\text{ }^\circ\text{C}$ . The oxygen partial pressure, which is controlled by the  $O_2$  flow rate of the assistant beam, is the main tuning parameter for ZITO films growth.  $O_2$  flow rates of 0 sccm, 3 sccm, 5 sccm, and 7 sccm were used and the deposited corresponding films are referred to as ZITO-0, ZITO-3, ZITO-5, and ZITO-7 respectively. Deposition time is 40 min and work pressure is  $4.5 \times 10^{-4}$  Torr. The film thickness is about 100 nm, which is tested by an alpha-step 200 from Tencor Instruments. Other detailed parameters of ZITO film deposition are listed in Table 1.

### *2.2 ZITO film properties measurement*

Properties of ZITO films were characterized using films deposited on commercial glass slides. Electrical properties were carried out using Hall Effect measurements with films of Van der Pauw geometry. For optical properties, transmittance and reflectance spectra were measured in the spectral range from 200 nm to 2000 nm using a UV/Vis/IR Perkin-Elmer lambda 1050 spectrophotometer with the integrating sphere in the dual beam mode.

Cross-sectional morphology of the as-deposited and the  $360\text{ }^\circ\text{C}$ -annealed ZITO-0 films on p-GaAs substrates were examined using scanning electron microscope (SEM,

Hitachi S4800) and the elemental composition by energy dispersive spectroscopy (EDS). Microstructure of the as-deposited and the 360 °C-annealed ZITO-0 films on silica glass was examined by an RIGAKU: ATX-G x-ray diffractometer.

### *2.3 Contact patterns fabrication and Electrical contact properties measurement*

Interfacial contact properties were characterized using ZITO films deposited on n-InP and p-GaAs substrates. In order to examine the electrical contact properties, photolithography process was used to define contact patterns for transmission line model (TLM) measurements. Fabrication process flow can be seen elsewhere [16] and the contact pattern illustration is shown in Fig.1. Parallel arrays of 4000 µm by 100 µm rectangle bars with various gap distances apart: 50 µm, 100 µm, 150 µm, 200 µm, 300 µm, 400 µm and 500 µm. Ti/Au (10 nm/300 nm) was then deposited by E-beam evaporation followed by a lift-off process to form metal contacts on ZITO. Finally, using the deposited metal pads as a self-alignment mask, the exposed ZITO film was removed using RIE in Methane/H<sub>2</sub>/Ar Plasma (CH<sub>4</sub>:H<sub>2</sub>:Ar=10:30:10 sccm, 50 mtorr, 200 W) to form ZITO islands and complete the fabrication process.

Electrical current-voltage (I-V curve) characteristics between ZITO films with n-InP and p-GaAs substrates were measured by standard two-probe measurement method using a Kiethley 2400 source meter. Before the electrical contact of ZITO films to n-InP and p-GaAs was tested, Ohmic contact of ZITO-0 film to Ti/Au was verified, shown in Fig.2.

### *2.4 Rapid Contact Annealing Process*

Rapid contact annealing processes (RCP) were carried out using a Jet First 100/150 Rapid Thermal Process, at 360 °C, 400 °C and 450 °C. Annealing duration is 60 seconds, while the temperature was raised rapidly in 10 seconds in forming gas (20% H<sub>2</sub>, balance

N<sub>2</sub>).

### 3. Results and discussion

#### 3.1 Properties of ZITO films

Electrical and optical properties of ZITO films prepared at different O<sub>2</sub> flow rates are concisely summarized in Table 2. It can be seen that with increasing the O<sub>2</sub> flow rate during film deposition, the carrier concentration (n) decreases from  $2.49 \times 10^{20} \text{ cm}^{-3}$  for ZITO-0 film to  $5.44 \times 10^{18} \text{ cm}^{-3}$  for ZITO-7 film. As the O<sub>2</sub> partial pressure increases, the carrier concentration decreases either by the removal of uncompensated oxygen vacancies, which can serve as intrinsic donor defects, or by the addition of oxygen interstitials, which can serve as compensating acceptor defects to donor dopants [22]. Due to the reduction of the carrier concentration, the Hall mobility ( $\mu$ ) of ZITO films increases with the increasing O<sub>2</sub> flow rate. Given that  $\sigma = n\mu e$ , the conductivity is highest at 525.2 S/cm for ZITO-0 film, while for ZITO-7 film the conductivity is 16.7 S/cm, which are consistent with A. Ambrosini's results [6], but much lower than D. Bruce Buchholz's [10].

Fiber-optic communication transmission C-band around 1550 nm are most widely-used, which have the lowest attenuation loss and achieve the longest range. Therefore, in this study, optical constants (refractive index n, absorption coefficient k and optical loss coefficient  $\alpha$ ) at 1550 nm are extracted from the transmittance and reflectance spectra of ZITO films, shown in Fig.3. It can be seen that the optical transmittance of ZITO in the visible and near-IR regions is about 75%-90%, which is consistent with reported [10, 23]. Additionally, the fundamental absorption edges of ZITO generally lie in the UV and shift

to shorter wavelengths with lower O<sub>2</sub> flow rate, due to the Moss-Burstein shift induced by the increasing carrier concentration [24]. The filling of excessive carriers in the conduction band leads to the increase of the optical band gap energy.

To remove the reflection and interference effects between glass substrates and ZITO films, the measured transmittance of ZITO films were corrected by T/1-R [15, 23]. Fig.4 is the illustration of the correction for ZITO-3 film, from which it can be seen that after corrected, interference fringes resulted from the reflection disappeared. All optical constants are calculated from corrected transmittance of ZITO films, shown in Table 2. The refractive index *n* at the wavelength of 1550 nm increases from 1.32 to 1.92 in dependence of the increasing O<sub>2</sub> flow rate during film deposition, because of the more sufficient oxidation. It should be noted that the refractive index of ZITO-0 film is extremely low as 1.32, which means big refractive index contrast between ZITO and n-InP or p-GaAs is obtained and strong confinement of light will be achieved as cladding material. Optical loss  $\alpha$  at 1550 nm was calculated using the relation  $\alpha = -\frac{1}{d} \ln T_{film}$ , where *d* is the film thickness, about 100 nm. It is highest for ZITO-0 film at 9775.3 cm<sup>-1</sup> and lowest for ZITO-7 film at 592.7 cm<sup>-1</sup>, where higher loss at higher carrier concentration results from free carrier absorption and free carrier scattering.

Optical band gap of ZITO films is estimated using the graph of  $(\alpha h\nu)^{1/2}$  versus *hν* [10,23] (as shown in Fig.5), where  $\alpha$  is the optical loss coefficient at energy *hν*. It is shown the optical band gap decreases with the decreasing carrier concentration from 3.61 eV for ZITO-0 film to 3.56 eV for ZITO-7 film, which results from the band filling effect, also known as the Burstein-Moss shift [24]. In addition, comparing with the un-

doped  $\text{In}_2\text{O}_3$  films [16], the optical band gap of ZITO is lower because of the bandgap narrowing, known as many-body effect [5].

### 3.2 Cross-sectional morphology and XRD of ZITO films

SEM spectrums of the as-deposited and the 360 °C- annealed ZITO-0 films deposited on  $\text{H}_2$ -cleaned p-GaAs were shown in Fig.6. The results show that the as-deposited film prepared by IAD is smooth and dense and grains are fine. The film thickness is about 100 nm. While after annealed at 360 °C, grains grow bigger with size about 50 nm and the film is dense but the film roughness increases. In addition, the interface between ZITO-0 film and  $\text{H}_2$ -cleaned p-GaAs is not smooth and clear after annealed, suggesting interdiffusion happens. Also, EDS results about the composition of ZITO-0 film reveal that In: Zn: Sn is 3.2:1.2:1 by at%, very close to the target composition, suggesting about 40% of the indium in the  $\text{In}_2\text{O}_3$  structure is replaced by substitution with zinc and tin in equal molar proportions:  $\text{In}_{2-2x}\text{Zn}_x\text{Sn}_x\text{O}_{3-6}$ , where  $x \approx 0.4$ , is the exact solubility limit for both zinc and tin in  $\text{In}_2\text{O}_3$  structure [5, 6].

Fig.7 shows XRD spectrum of the as-deposited and the 360°C-annealed ZITO-0 films coated on silica glasses, suggesting that both the as-deposited and the 360°C-annealed ZITO-0 films are amorphous. M. S. Grover's study [23] showed the fact that ZITO is a multicomponent oxide semiconductor system ensures that the structure remains amorphous under a wide range processing conditions.

### 3.3 Electrical Contact property of ZITO films to n-InP

Fig.8 shows I-V curves of ZITO film contacts to n-InP with different  $\text{O}_2$  flow rates during film deposition: (a) solvent-cleaned substrates; (b)  $\text{O}_2$ -cleaned substrates; (c)  $\text{H}_2$ -cleaned substrates. For solvent-cleaned substrates as shown in Fig.8 (a), no standard

Ohmic contact was achieved. When the O<sub>2</sub> flow rate was 0 sccm, the sample showed standard Schottky behavior, but when the O<sub>2</sub> flow rate was increased as 3 sccm, 5 sccm and 7 sccm, approximate Ohmic contacts were observed. For O<sub>2</sub>-cleaned substrates as shown in Fig.8 (b), Ohmic contacts were achieved when the O<sub>2</sub> flow rates are 0 sccm and 7 sccm and Schottky contacts were observed with the O<sub>2</sub> flow rates of 3 sccm and 5 sccm.

For H<sub>2</sub>-cleaned substrates as shown in Fig.8 (c), all ZITO film contacts to n-InP showed Ohmic behavior. What's more, Fig.8 (d) showed corresponding dynamic resistances of ZITO film contacts to H<sub>2</sub>-cleaned n-InP, which were calculated from their I-V curves. It can be seen that when the O<sub>2</sub> flow rates are 3 sccm and 7 sccm, the dynamic resistances are small and the biggest dynamic resistance was observed at 5 sccm.

We estimate barrier heights ( $q\Phi_{Bn}$ ) of the contacts, which is related to the Padovani-Stratton parameter defined by

$$E_{00} = \frac{q\hbar}{2} \sqrt{\frac{N_d}{m^* \varepsilon}}$$

where  $N_d$  is the donor concentration,  $\hbar$  is the reduced Plank constant,  $m^*$  is the effective mass of electron and  $\varepsilon$  is the dielectric permittivity of n-InP. The ratio  $E_{00}/k_bT$  gives an indication of the electron transport mechanism of TE ( $E_{00}/k_bT \ll 1$ ), TFE ( $E_{00}/k_bT \sim 1$ ) or FE ( $E_{00}/k_bT \gg 1$ ) [25]. In our case, a comparison of  $E_{00}$  to  $k_bT$  shows that TE mechanism is the dominant carrier transport process at the ZITO film/n-InP ( $N_d=7.00 \times 10^{17} \text{ cm}^{-3}$ ) interfaces. Therefore, the calculated  $q\Phi_{Bn}$  values of these samples were obtained according to Bethe's thermionic emission theory [26], which are summarized in Table 3.

From Table 3, it can be seen that for solvent-cleaned samples, the barrier height monotonously gets lower with the increasing O<sub>2</sub> flow rate, 0.688 eV for ZITO-7 film contact to n-InP corresponding to its approximate Ohmic contact (seen in Fig.8 (a)). For O<sub>2</sub>-cleaned samples, when the O<sub>2</sub> flow rates were 3 sccm and 5 sccm, contacts of ZITO film to n-InP show much greater barrier height than the solvent-cleaned counterparts, corresponding to their Schottky behavior (seen in Fig.8 (b)), which agrees well with Milliron's study [20] and Wu's study [21] about the activation effect of O<sub>2</sub> plasma treatment on semiconductors by improving the surface work function. But when the O<sub>2</sub> flow rates were 0 sccm and 7 sccm, contacts show really low barrier heights and standard Ohmic contacts were observed (seen in Fig.8 (b)). We know ZITO-0 film possesses the highest oxygen vacancies and ZITO-7 film possesses the highest oxygen concentration. The fact that Ohmic contacts happen to ZITO-0 film and ZITO-7 film, while Schottky behavior happens to ZITO-3 film and ZITO-5 film, indicates the oxygen state in ZITO film plays a key role in its contact to O<sub>2</sub>-cleaned n-InP. Comparing with both the solvent-cleaned and the O<sub>2</sub>-cleaned samples, barrier heights of H<sub>2</sub>-cleaned samples are all much lower, corresponding to their Ohmic behavior (seen in Fig.8 (c)), suggesting that H<sub>2</sub> plasma pretreatment to n-InP can lower the contact barrier height and is conducive to form Ohmic contact due to its passivation effect on the substrate surface, which is in good agreement with Huang's study on contact of Ti and 4H-SiC [27]. But ZITO-5 film contact to H<sub>2</sub>-cleaned n-InP shows a higher barrier height than other three ZITO-0, ZITO-3 and ZITO-7 films.

According to the classic metal-semiconductor contact theory, in order to achieve Ohmic contact between a TCO film and an n-type nondegenerate semiconductor, it is

required that the Fermi level of the TCO be less than that of the semiconductor [28]. ZITO films will possess higher work function with higher O<sub>2</sub> flow rates during film deposition, originating from the lower carrier concentration of the films (shown in Table 2). While for solvent-cleaned samples, the barrier height of ZITO film contacts to n-InP substrate decreases with the increasing O<sub>2</sub> flow rate, which means, for ZTIO film contacts to solvent-cleaned n-InP, work function of ZITO films has little effect on the barrier height of the contacts and the interfacial state is the key factor. When the n-InP substrates were pretreated by H<sub>2</sub> or O<sub>2</sub> plasma, Ohmic contacts were achieved, which also approves that.

Comparing with our previous study [16] on un-doped In<sub>2</sub>O<sub>3</sub> film contacts to n-InP, where monotonous change rules were observed: with the increasing O<sub>2</sub> flow rate, the contact barrier height increases for solvent-cleaned samples, which follows the classic metal-semiconductor contact theory; for H<sub>2</sub>-cleaned and O<sub>2</sub>-cleaned ones, results agree well with the passivation effect of H<sub>2</sub> plasma and the activation effect of O<sub>2</sub> plasma, in this paper on ZITO film contacts to n-InP, things are complicated: only for solvent-cleaned samples, the contact barrier height decreases monotonously with the increasing O<sub>2</sub> flow rate, which doesn't follow the classic metal-semiconductor contact theory; while for H<sub>2</sub>-cleaned and O<sub>2</sub>-cleaned samples, no obvious change rules can be obtained. So, it can be concluded it is the multicomponent of ZITO that causes things complicated. But details are not clear now and further researches on contact of TCO films to semiconductors are needed.

Specific contact resistivities of ZITO film contacts to H<sub>2</sub>-cleaned n-InP were calculated from their dynamic resistances with TML method. Besides the ZITO film/n-

InP substrate interfacial contact resistance, the dynamic resistance as calculated from I-V curve is the total resistance also including the resistances due to the test circuit, the probes, the metal pads, the ZITO film, the InP substrate, and the probe/metal and the metal/ ZITO interfaces. The resistances due to the test circuit, the probes, the metal pads and the probe/metal pad interfaces can be calculated from the tested I-V curves when the two testing probes are placed in one testing bar of the contact pattern (seen in Fig.1), which is 1.79  $\Omega$ . In addition, contact of the metal pads to ZITO film is verified to be Ohmic, seen in Fig.2. So, resistances due to the metal/ ZITO film interfaces and the ZITO film itself can be negligible, in consideration of the good conductivity of ZITO-0 films. Now, only the ZITO film/n-InP substrate interfacial contact resistance and the n-InP substrate resistance are left, which follows the structure of TML presented by E. F. Schubert [29]. The specific contact resistivities are calculated as  $1.84 \times 10^{-4} \Omega \cdot \text{cm}^2$ ,  $1.52 \times 10^{-6} \Omega \cdot \text{cm}^2$ ,  $7.42 \times 10^{-3} \Omega \cdot \text{cm}^2$  and  $1.60 \times 10^{-6} \Omega \cdot \text{cm}^2$  for ZITO-0 film, ZITO-3 film, ZITO-5 film and ZITO-7 film contacts to H<sub>2</sub>-cleaned n-InP, respectively.

Though the as-deposited ZITO-3 film and ZITO-7 film contacts to H<sub>2</sub>-cleaned n-InP possess lower specific contact resistivities, the ZITO-0 film contacts to both H<sub>2</sub>-cleaned and O<sub>2</sub>-cleaned n-InP substrates show good contact thermal stability during the following RCP, shown in Fig.9. The specific contact resistivities of ZITO-0 film contacts to both H<sub>2</sub>-cleaned and O<sub>2</sub>-cleaned n-InP in the following RCP were also calculated with TML method. For H<sub>2</sub>-cleaned n-InP substrates, the specific contact resistivities of ZITO-0 films are  $1.84 \times 10^{-4} \Omega \cdot \text{cm}^2$ ,  $7.5 \times 10^{-4} \Omega \cdot \text{cm}^2$ ,  $7 \times 10^{-4} \Omega \cdot \text{cm}^2$  and  $1.24 \times 10^{-4} \Omega$  for as-deposited, 360 °C-annealed, 400 °C-annealed and 450 °C-annealed samples respectively, which first shows an increasing trend and then decreases with the increasing annealing

temperature. For O<sub>2</sub>-cleaned n-InP substrates, the specific contact resistivities of ZITO-0 films are  $1.79 \times 10^{-5} \Omega \cdot \text{cm}^2$ ,  $4.32 \times 10^{-4} \Omega \cdot \text{cm}^2$ ,  $1.63 \times 10^{-3} \Omega \cdot \text{cm}^2$  and  $4.64 \times 10^{-3} \Omega \cdot \text{cm}^2$  for as-deposited, 360 °C -annealed, 400 °C -annealed and 450 °C -annealed samples respectively, which shows a monotonic increasing trend with the increasing annealing temperature, probably because the oxide interlayer induced by O<sub>2</sub> plasma treatment gets thicker in RCP and the contact barrier increases [15]. So, the electrical contact property of ZITO-0 film contact to H<sub>2</sub>-cleaned n-InP substrate has better thermal stability than O<sub>2</sub>-cleaned ones and the passivation effect of H<sub>2</sub> plasma will not weaken even after contact annealing process high at 450 °C.

#### *3.4 Electrical Contact property of ZITO films to p-GaAs*

The electrical contact property of ZITO films to p-GaAs substrates was also studied and their I-V curve measurements in dependence of the O<sub>2</sub> flow rate during film deposition are shown in Fig.10. It can be seen that for all as-deposited ZITO film contacts to solvent-cleaned, H<sub>2</sub>-cleaned and O<sub>2</sub>-cleaned p-GaAs substrates show Schottky behavior and their barrier height are all higher than those to n-InP substrates (seen in Fig.8), suggesting that it is more difficult for ZITO film forming Ohmic contact to p-GaAs, and for as-deposited samples, H<sub>2</sub> and O<sub>2</sub> plasma pretreatments to p-GaAs are not effective to achieve Ohmic contact.

While after RCP at 360 °C and 400 °C, Ohmic contacts of ZITO-0 films to H<sub>2</sub>-cleaned p-GaAs were achieved, shown in Fig.11. Comparing with the as-deposited ZITO-0 film contact to H<sub>2</sub>-cleaned p-GaAs, the contact barrier decreases sharply after annealed. Though when the annealing temperatures are 360 °C and 400 °C, Ohmic contacts were achieved, Schottky behavior was observed when the annealing temperature was increased

to 450 °C. Studies [30, 31] have shown that during annealing process, GaO<sub>x</sub> interlayer will be produced because of the interdiffusion of the film and the substrate. The existence of such oxide interlayer will increase the contact barrier, but meanwhile more Ga vacancies will be produced on the surface of the substrate. And high vacancy concentration means high electrical current of the tunneling effect between the TCO film and the GaAs substrate. So after annealed at proper temperature, contact resistance will be decreased on some level. But when the annealing temperature is too high, thickness of such GaO<sub>x</sub> interlayer will get increased and the interfacial electrical property will be deteriorated.

The specific contact resistivities of the 360 °C-annealed and the 400 °C-annealed ZITO-0 films to H<sub>2</sub>-cleaned p-GaAs were calculated with TML method, which are  $2.01 \times 10^{-2} \Omega \cdot \text{cm}^2$  and  $2.12 \times 10^{-2} \Omega \cdot \text{cm}^2$ , respectively. Comparing with contacts of ZITO-0 film to H<sub>2</sub>-cleaned n-InP (seen in Fig.9), such specific contact resistivities are much higher.

#### 4. Conclusions

Equal-cosubstituted ZITO films were prepared by IAD and H<sub>2</sub> or O<sub>2</sub> plasma treatments to n-InP and p-GaAs substrates prior to film deposition and O<sub>2</sub> flow rate during film deposition were tuned. Highest conductivity at 525.2 S/cm, highest optical loss at 9775.3 cm<sup>-1</sup> and lowest refractive index at 1.32 at 1550 nm for ZITO-0 film were obtained. Contacts of ZITO-0 films to both H<sub>2</sub>-cleaned and O<sub>2</sub>-cleaned n-InP substrates show Ohmic behavior and the contact of as-deposited ZITO-0 film to H<sub>2</sub>-cleaned n-InP possesses low specific contact resistivity at  $1.84 \times 10^{-4} \Omega \cdot \text{cm}^2$  and better thermal stability than O<sub>2</sub>-cleaned ones in the rapid contact annealing process, and its specific contact

resistivity remains  $1.24 \times 10^{-4} \Omega \cdot \text{cm}^2$  after annealed at 450 °C. What's more, Ohmic contacts were also achieved for ZITO-0 films to H<sub>2</sub>-cleaned p-GaAs after annealed at 360 °C and 400 °C, but their specific contact resistivities are high as  $2.01 \times 10^{-2} \Omega \cdot \text{cm}^2$  and  $2.12 \times 10^{-2} \Omega \cdot \text{cm}^2$ , respectively.

## Acknowledgements

Use of the Center for Nanoscale Materials was supported by the U. S. Department of Energy, Office of Science, Office of Basic Energy Sciences, under Contract No. DE-AC02-06CH11357.

## References

- [1] H. Enoki, T. Nakayama, and J. Echigoya, The intermediate compound in the In<sub>2</sub>O<sub>3</sub>-SnO<sub>2</sub> system. *Phys. Status Solidi A*, 1992, 129, 181.
- [2] T. Minami, S. Takata, T. Kakumu, and H. Sonohara, Physics of very thin ITO conducting films with high transparency prepared by DC magnetron sputtering. *Thin Solid Films*, 1995, 270 (1-2), 22.
- [3] Gordon R.G., Preparation and properties of transparent conductors. *Mat. Res. Soc. Sym. Proc.*, 1996, 426, 419-429.
- [4] Tadatsugu Minami, New n-Type Transparent Conducting Oxides. *Mrs Bulletin*, 2000, 38-44.
- [5] G. B. Palmer, K. R. Poepelmeier, T. O. Mason, Conductivity and Transparency of ZnO/SnO<sub>2</sub> Cosubstituted In<sub>2</sub>O<sub>3</sub>. *Chem. Mater.* 1997, 9, 3121.

- [6] A. Ambrosini, G. B. Palmer, A. Maignan, K. R. Poeppelmeier, M. A. Lane, P. Brazis, C. R. Kannewurf, T. Hogan and T. O. Mason, Variable-Temperature Electrical Measurements of Zinc Oxide/Tin Oxide-Cosubstituted Indium Oxide. *Chem. Mater.* 2002, 14, 52.
- [7] Frank G., Brock L., Bausen H., The solubilities of Sn in  $\text{In}_2\text{O}_3$  and of In in  $\text{SnO}_2$  crystals grown from Sn-In melts. *J. Cryst. Growth*, 1976, 36, 179.
- [8] Nakamura M., Kimizuka N., Mohri, T., The phase relations in the  $\text{In}_2\text{O}_3\text{-Fe}_2\text{ZnO}_4\text{-ZnO}$  system at 1350°C. *J. Solid State Chem.*, 1990, 86, 16.
- [9] M. Zhang, D.B. Buchholz, S.J. Xie, R.P.H. Chang, Twinned domains in epitaxial  $\text{ZnO/SnO}_2$ -cosubstituted  $\text{In}_2\text{O}_3$  thin films. *Journal of Crystal Growth*, 2007, 308, 376.
- [10] D. Bruce Buchholz, Jun Liu, Tobin J. Marks, Ming Zhang, Robert P. H. Chang, Control and Characterization of the Structural, Electrical, and Optical Properties of Amorphous Zinc-Indium-Tin Oxide Thin Films. *ACS Applied Materials and Interfaces*, 2009, 1(10), 2147.
- [11] Kyung-Han Seo, Joon-Hyung Lee, Jeong-Joo Kim, Sintering behaviors and electrical properties of transparent conducting  $\text{In}_6\text{Sn}_{2-x}\text{Zn}_x\text{O}_{13-x}$  ceramics with different Sn/Zn ratio. *J. Electroceram*, 2006, 17, 1057.
- [12] Julia M. Phillips, R. J. Cava, G. A. Thomas, et.al., Zinc-indium-oxide: A high conductivity transparent conducting oxide. *Applied Physics Letters*, 1995, 67, 2246.
- [13] Nakamura, M., Nunoya, N., Morshed, M., Tamura, S., Arai, S., Very low threshold current density operation of 1.5  $\mu\text{m}$  DFB lasers with wire-like active regions. *IET Electronics Letters*, 2001, 36 (7), 639-640.
- [14] Minami, T., Transparent conducting oxide semiconductors for transparent

- electrodes. *Semicond. Sci. Technol.* 2005, 20, S35-S44.
- [15] Fang Ou, D. Bruce Buchholz, Fei Yi and etc. Ohmic Contact of Cadmium Oxide, a Transparent Conducting Oxide, to n-type Indium Phosphide. *ACS Appl. Mater. Interfaces*, 2011, 3, 1341-1345.
- [16] Xiufeng Tang, Chunhan Hseih, Fang Ou and Seng-Tiong Ho, Ohmic contact of indium oxide as transparent electrode to n-type indium phosphide. *RSC Adv.* 2015, 5, 22685-22691.
- [17] Carrie Donley, Darren Dunphy, David Paine, and etc. Characterization of Indium-Tin Oxide Interfaces Using X-ray Photoelectron Spectroscopy and Redox Processes of a Chemisorbed Probe Molecule: Effect of Surface Pretreatment Conditions. *Langmuir*, 2002, 18, 450-457.
- [18] Hiroyuki Hirayama, Toru Tatsumi, Hydrogen passivation effect in Si molecular beam epitaxy, *Applied Physics Letters*, 1989, 54: 1561.
- [19] B. Anthony, T. Hsu, L. Breaux, R. Qian, S. Banerjee and A. Tasch, Very Low Defect Remote Hydrogen Plasma Clean of Si (100) for Homoepitaxy, *Journal of Electronic Materials*, 1990, 19 (10): 1027-1032.
- [20] Milliron, D. J.; Hill, I. G.; Shen, C.; Kahn, A.; Schwartz, J., Surface oxidation activates indium tin oxide for hole injection. *J. Appl. Phys.* 2000, 87, 572-576.
- [21] Wu, C. C.; Wu, C. I.; Sturm, J. C.; Kahn, A., Surface modification of indium tin oxide by plasma treatment: An effective method to improve the efficiency, brightness, and reliability of organic light emitting devices. *Appl. Phys. Lett.* 1997, 70, 1348-1350.
- [22] Ingram, B. J. ; Gonzalez, G. B. ; Kammler, D. R. ; Bertoni, M. I. ; Mason, T.O. ,

- Chemical and Structural Factors Governing Transparent Conductivity in Oxides. *J. Electroceram.*, 2004, 13, 167-175.
- [23] M. S. Grover, P. A. Hersh, H. Q. Chiang, E. S. Kettenring, J. F. Wager and D. A. Keszler, Thin-film transistors with transparent amorphous zinc indium tin oxide channel layer. *J. Phys. D: Appl. Phys.*, 2007, 40, 1335-1338.
- [24] E. Burstein, Anomalous Optical Absorption Limit in InSb. *Phys. Rev.*, 1954, 93, 632.
- [25] S. M. Sze, *Physics of Semiconductor Device*, 2nd ed., Wiley, New York, 1981.
- [26] A. Bethe, Theory of the boundary layer of crystal rectifiers, MIT Radiation Lab Report, 1942, 43: 12-15.
- [27] Lingqin Huang, Bingbing Liu, Qiaozhi Zhu, Suhua Chen, Mingchao Gao, Fuwen Qin, and Dejun Wang, Low resistance Ti Ohmic contacts to 4H-SiC by reducing barrier heights without high temperature annealing, *Applied Physics Letters*, 2012, 100, 263503.
- [28] Blank, T.V.; Gol'dberg, Y. A. Mechanisms of current flow in metal-semiconductor ohmic contacts. *Semiconductors*, 2007, 41, 1263-1292.
- [29] E. F. Schubert, J. M. Shah, *Physical Foundations of Solid State Devices*, 2007.
- [30] J. O. Song, J. S. Kwak, Y. Park et al. Improvement of the light output of InGaN-based light-emitting diodes using Cu-doped indium oxide /indium tin oxide p-type electrodes. *Applied Physics Letters*, 2005, 86: 2135051~2135053.
- [31] K. M. Chang, J. Y. Chu, C. C. Cheng et al. Investigation of indium–tin-oxide ohmic contact to p-GaN and its application to high-brightness GaN-based light-emitting diodes. *Solid-State Electronics*, 2005, 49(8): 1381~1386.

**Figure and Table Captions:**

Fig.1 Pattern illustration of ZITO film contacts to n-InP and p-GaAs

Fig.2 I-V curve measurement of ZITO-0 film contact to Ti/Au

Fig.3 Transmittance and reflectance spectra of ZITO-0, ZITO-3, ZITO-5 and ZITO-7

Fig.4 Correction of the transmittance spectra of ZITO-3 film for reflection and film-substrate interference

Fig.5 Optical band gap of ZITO films in dependence of different O<sub>2</sub> flow rates

Fig.6 Cross-sectional SEM of ZITO-0 film on p-GaAs, (a) as-deposited; (b) 360°C-annealed

Fig.7 XRD spectrum of the as-deposited and 360°C-annealed ZITO-0 films

Fig.8 I-V curve measurements of ZITO film contacts to n-InP with different O<sub>2</sub> flow rates during film deposition: (a) solvent-cleaned; (b) O<sub>2</sub>-cleaned; (c) H<sub>2</sub>-cleaned; (d) calculated dynamic resistances of ZITO film contacts to H<sub>2</sub>-cleaned n-InP

Fig.9 I-V curve measurements of ZITO-0 film contacts to n-InP substrates after rapid contact annealing process, (a) H<sub>2</sub>-cleaned; (b) O<sub>2</sub>-cleaned

Fig.10 I-V curve measurements of ZITO film contacts to p-GaAs with different O<sub>2</sub> flow rates during film deposition: (a) solvent-cleaned; (b) H<sub>2</sub>-cleaned; (c) O<sub>2</sub>-cleaned

Fig.11 I-V curve measurements of ZITO-0 film contacts to H<sub>2</sub>-cleaned p-GaAs after rapid contact annealing process

Table 1 Parameters of ZITO film deposition by IAD

Table 2 Electrical and optical properties of ZITO films at different deposition conditions

Table 3 Barrier height ( $q\Phi_{bn}$ ) of as-deposited ZITO film contacts to n-InP

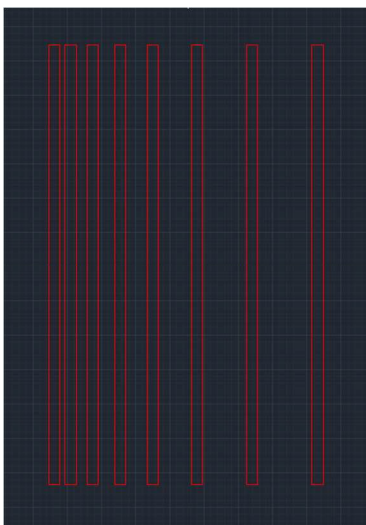


Fig.1 Pattern illustration of ZITO film contacts to n-InP and p-GaAs

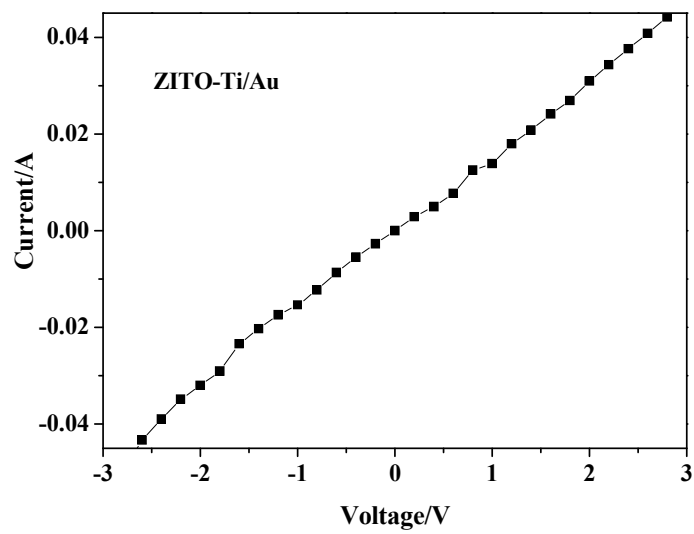


Fig.2 I-V curve measurement of ZITO-0 film contact to Ti/Au

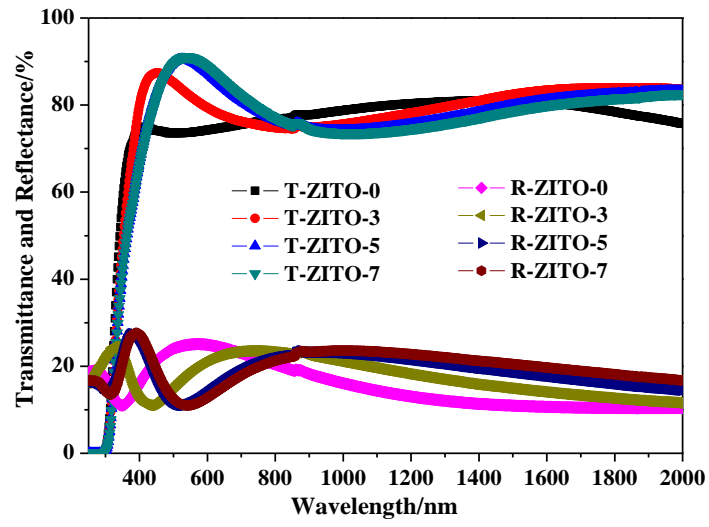


Fig.3 Transmittance and reflectance spectra of ZITO-0, ZITO-3, ZITO-5 and ZITO-7

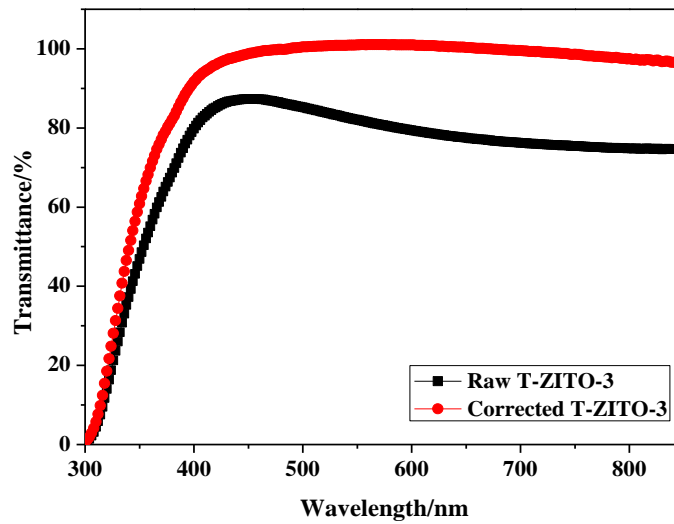


Fig.4 Correction of the transmittance spectra of ZITO-3 film for reflection and film-substrate interference

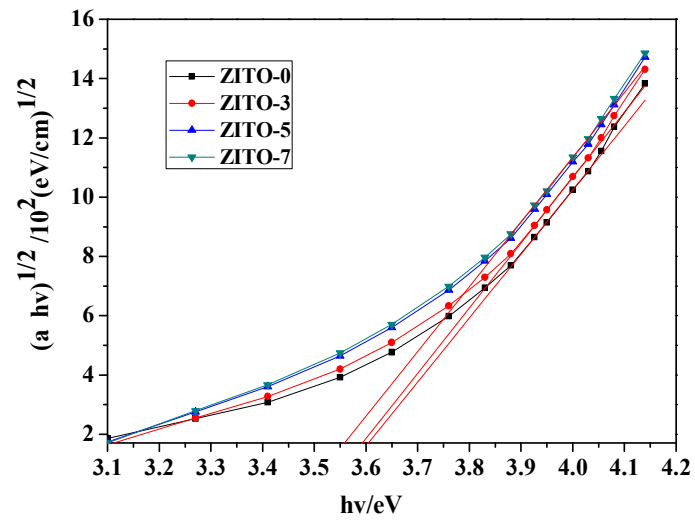


Fig.5 Optical band gap of ZITO films in dependence of different O<sub>2</sub> flow rates

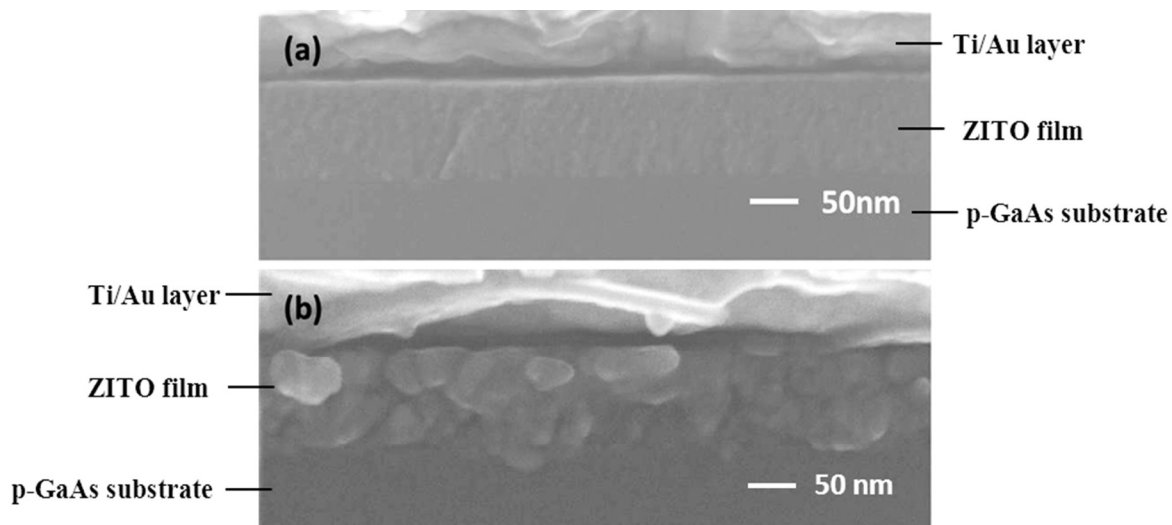


Fig.6 Cross-sectional SEM of ZITO-0 film on p-GaAs, (a) as-deposited; (b) 360°C-annealed

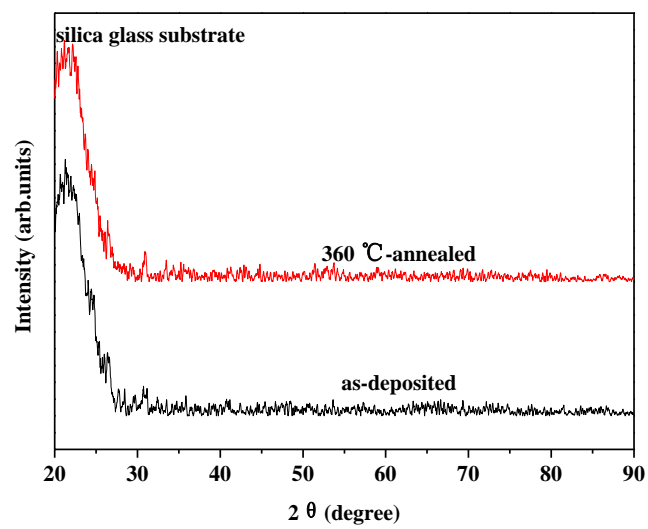


Fig.7 XRD spectrum of the as-deposited and 360°C-annealed ZITO-0 films

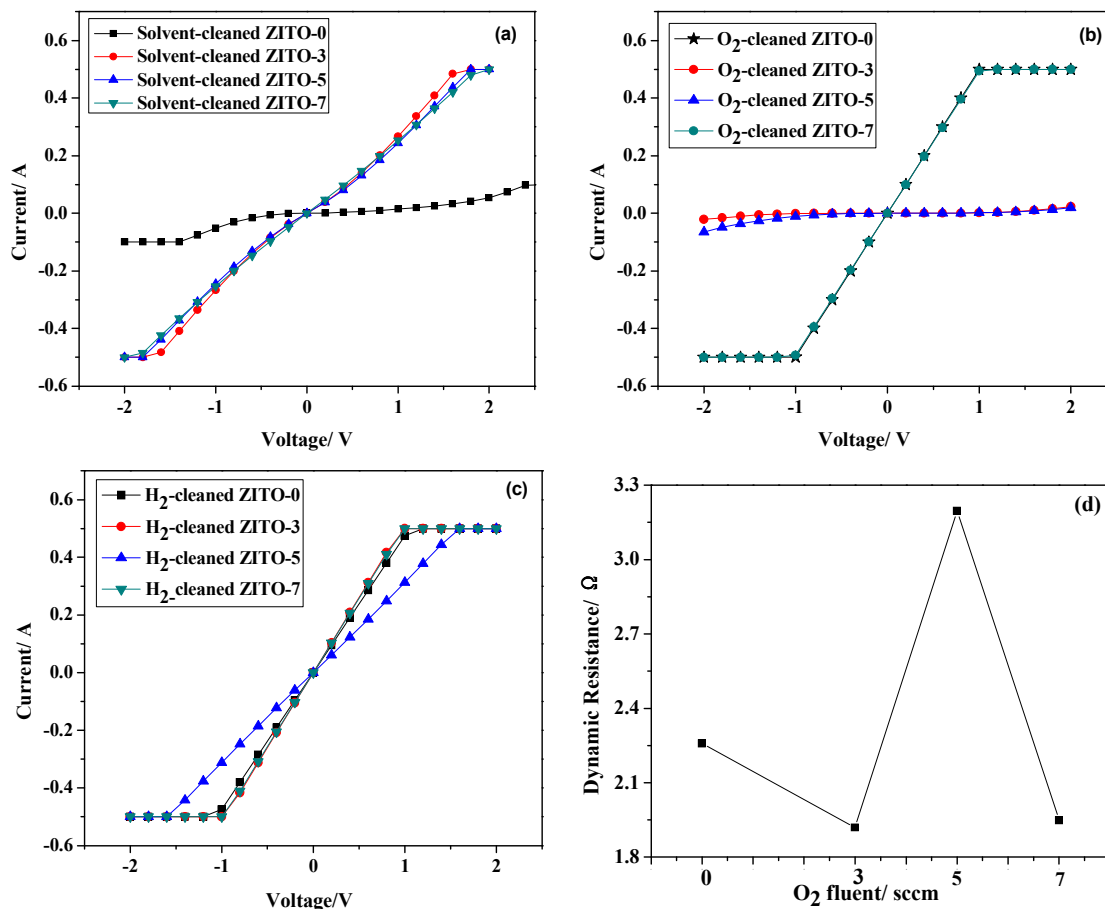


Fig.8 I-V curve measurements of ZITO film contacts to n-InP with different O<sub>2</sub> flow rates during film deposition: (a) solvent-cleaned; (b) O<sub>2</sub>-cleaned; (c) H<sub>2</sub>-cleaned; (d) calculated dynamic resistances of ZITO film contacts to H<sub>2</sub>-cleaned n-InP

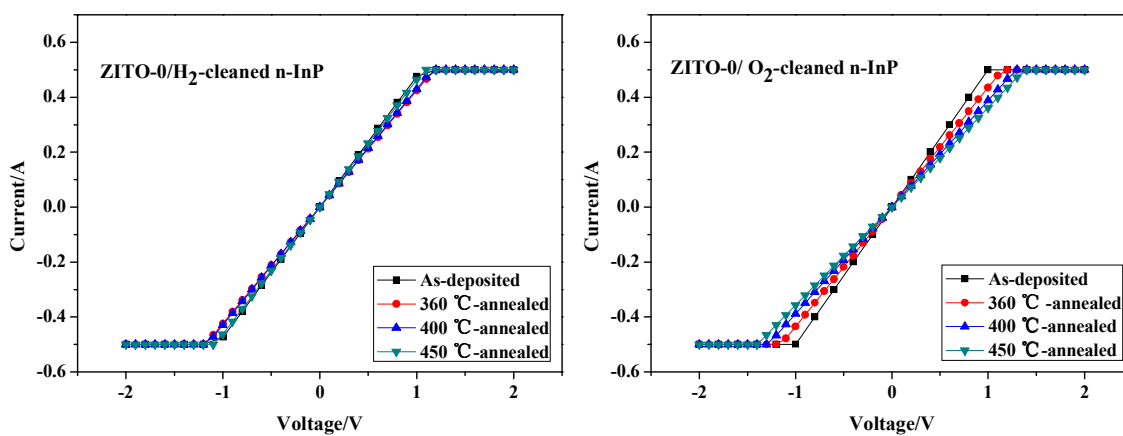


Fig.9 I-V curve measurements of ZITO-0 film contacts to n-InP substrates after rapid contact annealing process, (a) H<sub>2</sub>-cleaned; (b) O<sub>2</sub>-cleaned

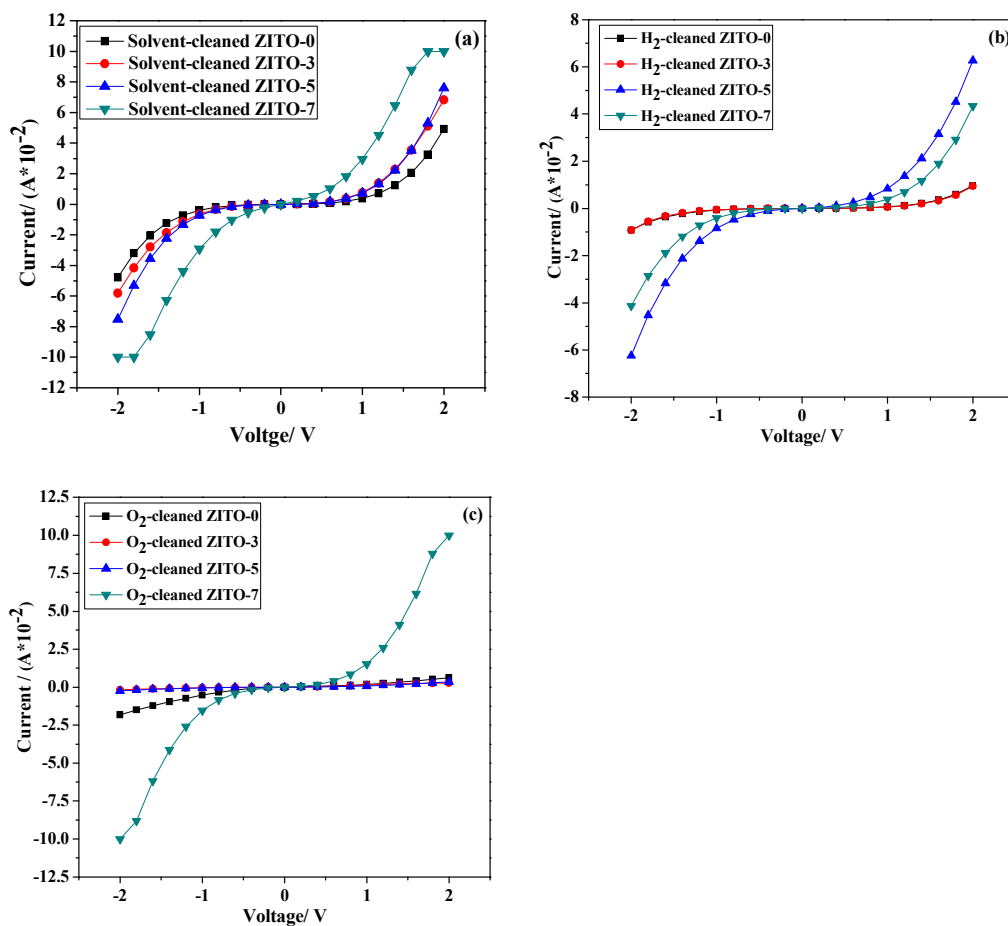


Fig.10 I-V curve measurements of ZITO film contacts to p-GaAs with different O<sub>2</sub> flow rates during film deposition: (a) solvent-cleaned; (b) H<sub>2</sub>-cleaned; (c) O<sub>2</sub>-cleaned

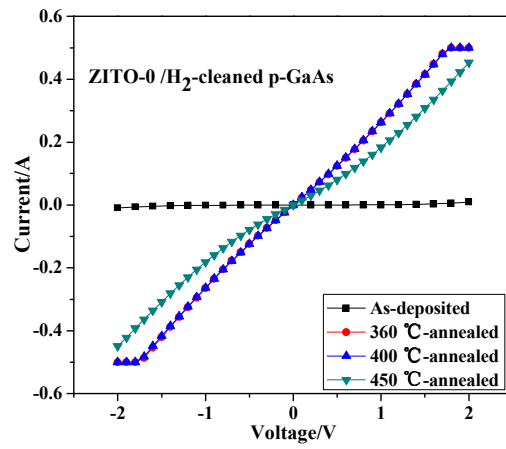


Fig.11 I-V curve measurements of ZITO-0 film contacts to H<sub>2</sub>-cleaned p-GaAs after rapid contact annealing process

Table 1 Parameters of ZITO film deposition by IAD

Main Beam						
Forward Power (W)	Beam Voltage (V)	Accelerate Voltage (V)	Beam Current (mA)	Argon Neutron (sccm)	Argon Source (sccm)	Oxygen (sccm)
230	1000	160	95	3	10	8
Assisted Beam						
Forward Power (W)	Beam Voltage (V)	Accelerate Voltage (V)	Beam Current (mA)	Argon Neutron (sccm)	Argon Source (sccm)	Oxygen (sccm)
98	200	350	35	3	10	0,3,5,7

Table 2 Electrical and optical properties of ZITO films at different deposition conditions

Deposition Condition (O <sub>2</sub> flow rate)	0	3	5	7
Carrier Concentration (cm <sup>-3</sup> )	2.49×10 <sup>20</sup>	5.32×10 <sup>19</sup>	2.72×10 <sup>19</sup>	5.44×10 <sup>18</sup>
Conductivity (S/cm)	525.2	186.9	92.5	16.7
Hall Mobility (cm <sup>2</sup> /Vs)	13.2	22.2	21.2	19.2
Complex Refr.Ind.@1550 nm (n+ik)	1.32+0.29 i	1.73+0.066 i	1.86+0.0416 i	1.92+0.0331 i
Optical Loss@ 1550 nm (cm <sup>-1</sup> )	9775.3	3096.7	1499.7	592.7
Optical Band Gap (eV)	3.61	3.59	3.56	3.56

Table 3 Barrier height ( $q\Phi_{Bn}$ ) of as-deposited ZITO film contacts to n-InP

n-InP	ZITO-0	ZITO-3	ZITO-5	ZITO-7
Solvent-cleaned	0.824 eV	0.697 eV	0.695 eV	0.688 eV
H <sub>2</sub> -cleaned	0.668 eV	0.668 eV	0.682 eV	0.668 eV
O <sub>2</sub> -cleaned	0.668 eV	0.925 eV	0.902 eV	0.668 eV